

Antiferromagnetic coupling between two adjacent dangling bonds on Si(001): Total-energy and force calculations

Ji Young Lee, Jin-Ho Choi, and Jun-Hyung Cho*

BK21 Program Division of Advanced Research and Education in Physics, Hanyang University, 17 Haengdang-Dong, Seongdong-Ku, Seoul 133-791, Korea

(Received 26 June 2008; published 14 August 2008)

Scanning tunneling microscopy experiments reported that desorption from the hydrogen- and halogen-terminated Si(001) surfaces exhibits frequently the two types of dangling-bond (DB) configurations. One is the intradimer configuration, where two DBs are within a single Si dimer, and the other is the interdimer configuration, where two DBs are on one side of two adjacent Si dimers. Our spin-polarized density-functional-theory calculations show that the intradimer configuration is nonmagnetic with a buckled-dimer geometry, while the interdimer configuration is antiferromagnetic with two adjacent symmetric dimers. In addition, we show that when the dissociative adsorption of hydrogen molecule occurs across the ends of two adjacent dimers on a clean Si(001) surface, such an antiferromagnetic coupling between two adjacent DBs still exists, thereby giving rise to a structural transformation from buckled to symmetric dimers.

DOI: 10.1103/PhysRevB.78.081303

PACS number(s): 75.70.Rf, 75.30.Et, 75.50.Ee

Dangling bonds (DBs) produced by hydrogen (halogen) desorption from the hydrogen(halogen)-terminated Si(001) -2×1 surface are essential for deposition, surface diffusion, oxidation, and etching processes.^{1,2} A detailed understanding of DB structures is prerequisite to exploiting chemically reactive DBs in various technological applications. The earlier model for the associative desorption of H₂ from the H-terminated Si(001) -2×1 surface was based on the intradimer reaction pathway because it provides a straightforward explanation for the observed first-order desorption kinetics via prepared H atoms on one Si dimer.^{3,4} However, it is now well established by a combination of scanning tunneling microscopy (STM) and nanosecond laser heating that the associative desorption of H₂ occurs through the interdimer reaction pathway, which involves H atoms from two adjacent Si dimers.^{4,5} Here, the initially formed interdimer configuration (containing two DBs on neighboring Si dimers; see Fig. 1) was observed to be converted into the intradimer configuration (containing a pair of DBs on the same dimer; see Fig. 1) via thermal diffusion of the adsorbed H atoms.⁴⁻⁶ Recently, it was reported⁷ that the desorption of halogen atoms from the halogen-terminated Si(001) -2×1 surfaces occurs via phonon activation of electrons into long-lived Si-halogen antibonding states. At the desorption temperatures, two generated single DBs diffuse to form a pair of DBs on the same dimer. Such an intradimer configuration can be converted into the interdimer configuration by adatom hopping induced by tunneling electrons of the STM.⁸ Thus, under tactical experimental conditions and atomic scale manipulation, the intradimer and interdimer configurations of DBs can be produced at the hydrogen- and halogen-terminated Si(001) surfaces.

The hitherto accepted structural models for the intradimer and interdimer configurations of DBs involve the buckling of Si dimers.^{9,10} The former configuration is composed of two buckled DBs on a single Si dimer and the latter one also contains the up and down displaced DBs because of the presence of two alternatively buckled dimers along the dimer row. However, despite the different heights of the two DBs in the interdimer configuration, the STM measurements at

~ 100 K showed two nearly equal bright protrusions in the filled-state image.¹¹ By considering that thermally activated flipping motion of buckled dimers becomes frozen at low temperatures below ~ 120 K,¹² the observed equal heights of the two DBs in the interdimer configuration may be associated with their static symmetric-dimer geometries rather than the flipping motion of buckled dimers. We here propose that the ground state of the interdimer configuration consists of symmetric dimers as a consequence of the antiferromagnetic coupling between two adjacent DBs, therefore providing an alternative explanation for the STM data.¹¹

In this work, we present a theoretical investigation of magnetic effects in the intradimer and interdimer configurations of DBs on the hydrogen- and halogen-terminated Si(001) surfaces within the spin-polarized density-functional theory (DFT). We find that the ground state of the intradimer configuration is nonmagnetic (NM), but that of the interdimer configuration is antiferromagnetic (AFM). Here, the electronic energy gain caused by spin polarization is found to be greater than that due to dimer buckling, leading to an

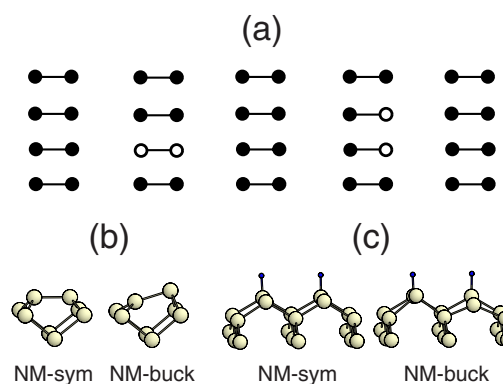


FIG. 1. (Color online) (a) Schematic top view of the intradimer and interdimer configurations. The filled (empty) circles represent H- or halogen-bonded (bare) Si atoms. The optimized NM-sym and NM-buck structures of the (b) intradimer and (c) interdimer configurations on H-terminated Si(001) are shown. The large (small) circles represent Si (H) atoms.

TABLE I. Desorption energies (in eV per H₂, 2Cl, or 2Br) and band gaps for the intradimer and inter-dimer configurations on H-, Cl-, and Br-terminated Si(001) surfaces. Desorption energy is defined as the energy cost of desorbing H₂ (two Cl or Br atoms) from the fill-covered Si(001)-(2×1) surface. Here, we used the total energy of spin-polarized free Cl and Br atoms. The band-gap energies (in eV) are given at the Γ point.

		H ₂		2Cl		2Br	
		E_{des}	E_{gap}	E_{des}	E_{gap}	E_{des}	E_{gap}
Intra	NM-sym	2.17	0.83	8.24	0.82	6.83	0.78
	NM-buck	2.03 (2.06 ^a ,2.03 ^b)	1.04	8.08	0.97	6.66	0.96
Inter	NM-sym	2.39	0.29	8.44	0.29	7.06	0.30
	NM-buck	2.36 (2.41 ^a ,2.41 ^b)	0.43	8.40	0.45	7.01	0.48
	FM	2.30	0.68	8.36	0.67	6.98	0.67
	AFM	2.24	0.85	8.29	0.83	6.91	0.84

^aReference 9.

^bReference 10.

AFM ground state for the interdimer configuration. We will show that such an AFM arrangement of the spins within two adjacent DBs appears even on a clean Si(001) surface as long as one side of two adjacent Si dimers is passivated by the dissociative adsorption of H₂.

The total-energy and force calculations were performed by using spin-polarized DFT (Ref. 13) within the generalized-gradient approximation.¹⁴ All atoms are described by norm-conserving pseudopotentials.¹⁵ The surface is modeled by a periodic slab geometry. Each slab contains six Si atomic layers plus one H (Cl or Br) atomic layer. The bottom Si layer is passivated by two H atoms per Si atom. The vacuum spacing between these slabs is about 8 Å. The electronic wave functions were expanded in a plane-wave basis set with a cutoff of 25 Ry. The \mathbf{k} -space integration was done with four points in the surface Brillouin zone of the 4 × 4 unit cell. All the atoms except the bottom two Si layers were allowed to relax along the calculated Hellmann-Feynman forces until all the residual force components were less than 1 mRy/bohr.

We start with a discussion of the intradimer configuration at the H-terminated Si(001) surface. Our spin-polarized DFT calculations show that both the symmetric-dimer and buckled-dimer structures are NM. Each of the optimized structures, designated as NM-sym and NM-buck, is shown in Fig. 1(b). The calculated desorption energies (E_{des}) of H₂ for these structures are compared with previous^{9,10} theoretical data in Table I. We find that NM-buck has $E_{\text{des}}=2.03$ eV, smaller than that (2.17 eV) of NM-sym. This result indicates that the former structure is energetically favored over the latter one by 0.14 eV. The greater stabilization of NM-buck compared to that of NM-sym is consistent with the conclusion, drawn from quantum Monte Carlo calculations¹⁶ on a clean Si(001) surface, that the buckled-dimer structure is lower in energy. In contrast with the NM ground state for the intradimer configuration, the interdimer configuration shows the presence of ferromagnetic (FM) and AFM couplings between two DBs. Here, the AFM structure is found to be favored over the FM, NM-buck, and NM-sym structures by $\Delta E=0.06$, 0.12, and 0.15 eV, respectively (see Table I). Thus, the ground state of the interdimer configuration is AFM. The

optimized NM-sym and NM-buck structures of the interdimer configuration are shown in Fig. 1(c). In the NM-sym structure, the height of the two H-unpassivated Si atoms is lowered by $\Delta h=0.06$ Å compared to that of the H-bonded Si atoms. We note that for the FM and AFM structures, this height difference Δh decreases to 0.04 Å, indicating that the presence of spin polarization would yield a slightly outward displacement of the two DBs. Therefore, we conclude that the FM and AFM structures of the interdimer configuration consist of two symmetric dimers.

Twenty years ago, based on an *ab initio* Hartree-Fock calculation, Artacho and Ynduráin¹⁷ proposed that the dimers on a clean Si(001) surface would be symmetric with an AFM spin arrangement within them. This proposal for symmetric dimers is consistent with geometries obtained from multiconfiguration self-consistent field and configuration interaction calculations on small clusters.¹⁸ However it is not supported by DFT calculations on slab geometries and large clusters as well as quantum Monte Carlo calculations.¹⁶ Interestingly, the present DFT calculations predict the existence of AFM coupling between two adjacent DBs in the interdimer configuration generated on the H-terminated Si(001) surface.¹⁹ Spin polarization in the interdimer configuration was discussed by Bird and Bowler,²⁰ who, however, concluded against an AFM ground state.

Figure 2 shows the calculated band structures for the intradimer and interdimer configurations on the H-terminated Si(001) surface. We find two surface-state bands, π and π^* , near the Fermi level. In the intradimer NM-sym (NM-buck) structure, the band gap between the π and π^* states is 0.83 (1.04) eV at the Γ point. Here, the increase in the band gap in NM-buck is due to a rehybridization of the dangling orbitals, accompanied by a charge transfer from the down to the up Si atom. As shown in Fig. 2(b), the charge characters of these surface states in NM-buck reveal that the π and π^* states represent dangling bonds which are localized at the up and down Si atoms, respectively. We note that the band gap in the interdimer NM-sym (NM-buck) structure is reduced to be 0.29 (0.43) eV, reflecting the reduced overlap of dangling orbitals with a relatively larger separation of two DBs. This rather localized feature of DBs in the interdimer configura-

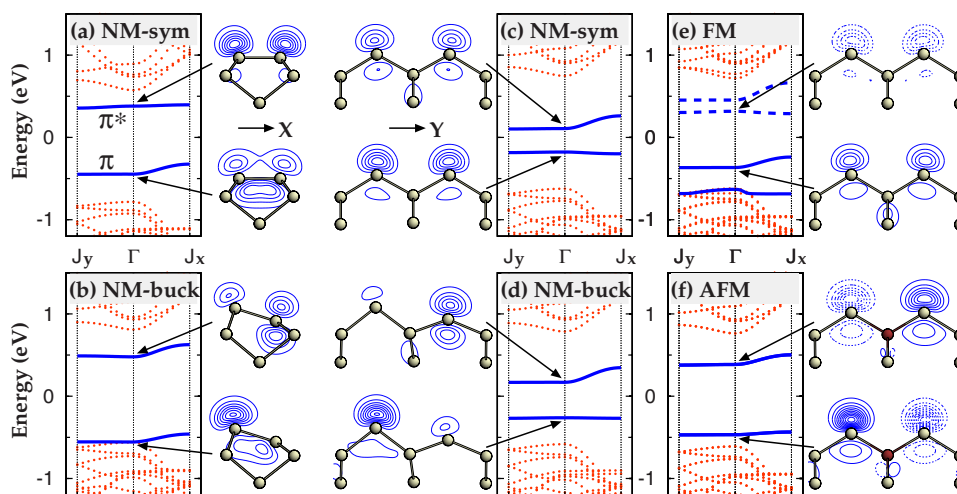


FIG. 2. (Color online) Calculated band structures of the intradimer and interdimer configurations on H-terminated Si(001). For the former configuration, (a) NM-sym and (b) NM-buck are displayed, while for the latter one, (c) NM-sym, (d) NM-buck, (e) FM, and (f) AFM are displayed. The energy zero represents the Fermi level. The direction of the Γ - J_x (Γ - J_y) line is perpendicular (parallel) to the Si dimer row. The charge characters of π and π^* states at the Γ point are also shown. In the contour plot, a uniform increment of 0.015 electron/ \AA^3 is used. In (e) and (f), the solid (dashed) line represents the positive (negative) spin density.

tion gives rise to the stabilization of spin polarization. The band gap in the interdimer FM (AFM) structure becomes 0.68 (0.85) eV [see Figs. 2(e) and 2(f)], larger than those in the interdimer NM-sym and NM-buck structures. Thus, we can say that in the interdimer configuration the electronic energy gain is greatly enhanced by generating spontaneous spin polarization, compared to by accompanying a Jahn-Teller lattice distortion.¹¹

From the energy difference between the FM and AFM structures, we estimate the exchange coupling constant between two spins in the interdimer configuration as 0.06 eV.²¹ This exchange coupling constant decreases to ~ 0.01 eV as two DBs are further separated to be on one side of next-nearest-neighbor dimers. Thus, it is likely that the AFM coupling between two DBs may be driven by a superexchange interaction via the bridging covalent-bonded subsurface and surface Si atoms.

To examine the existence of AFM coupling between two adjacent DBs on a clean Si(001) surface, we consider the dissociative adsorption of H_2 onto two neighboring Si dimers. Such an interdimer dissociation creating two single DBs is well known from both theory^{9,10} and experiment.^{4,22} Its optimized NM-buck and AFM structures are shown in Fig. 3. We find that AFM is more stable than NM-buck by 0.05 eV. This stabilization energy of AFM on clean Si(001)

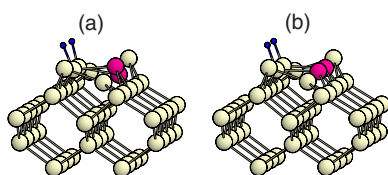


FIG. 3. (Color online) Optimized (a) NM-buck and (b) AFM structures for the dissociative adsorption of H_2 on Si(001). The large (small) circles represent Si (H) atoms. For distinction, the Si atoms containing a single DB are in gray.

is smaller than the corresponding one (0.12 eV) on H-terminated Si(001), implying that the AFM coupling of two spins in the former is weaker than that in the latter. This can be accounted for by the fact that DB orbitals in the former become less localized compared to those in the latter because of their interactions with π orbitals of neighboring H-unpassivated Si dimers.

Hitosugi *et al.*¹¹ performed STM studies on DB linear chains fabricated on the H-terminated Si(001)- 2×1 surface at low temperatures ranging from 96 to 110 K. In their filled-state STM image for the interdimer configuration, two DBs appeared symmetric with nearly equally bright protrusions. Especially, the cross-sectional view of the filled-state image along the line connecting the two DBs showed a peak-to-valley height difference of ~ 0.3 \AA .¹¹ Using the Tersoff-Hamann approximation,²³ we simulate the constant-current STM images for the filled and empty states of the interdimer configuration within the NM-buck and AFM structures. The results are displayed in Fig. 4. We find that the filled-state image of NM-buck has a single bright spot on the up displaced DB, while that of AFM shows two bright spots which are symmetric with respect to a plane bisecting the interdimer configuration. As shown in Fig. 4(b), the cross-sectional view of the filled-state image of AFM gives a peak-to-valley height difference of 0.47 \AA ,²⁴ close to the above measured value of ~ 0.3 \AA . Thus, assuming that the flipping motion of buckled dimers becomes frozen at ~ 100 K,¹² we can say that the observed¹¹ symmetric STM image of the interdimer configuration cannot be associated with the dynamics of NM-buck but with the static symmetric-dimer geometry of AFM.

We also study the structural and magnetic properties of the intradimer and interdimer configurations generated on the Cl- and Br-terminated Si(001) surfaces. As shown in Table I, the calculated desorption energies of halogen atoms are found to be significantly larger compared to those of H_2 because halogen atoms desorb atomically. However, the rela-

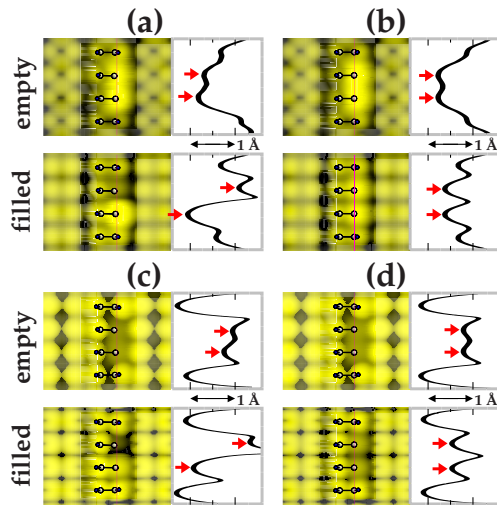


FIG. 4. (Color online) Simulated STM images of the interdimer configuration within (a) NM-buck and (b) AFM on H-terminated Si(001), including the cross-sectional view along the line connecting two DBs. The results for the interdimer (c) NM-buck and (d) AFM on Br-terminated Si(001) are also given. All the empty-state images are obtained by integrating the charge from E_F to $E_F + 1.5$ eV, whereas the filled-state images for H(Br)-terminated Si(001) are obtained from $E_F - 2.0$ eV ($E_F - 1.0$ eV) to E_F . Here, the different bias voltages are used for comparison with experiments (Refs. 8 and 11). All the images were taken at $\rho = 7 \times 10^{-5}$ electrons/Å³. The arrows indicate the positions of DBs.

tive energy differences among various structures are similar between the halogen- and H-terminated Si(001) cases, leading to the same conclusions about the NM (AFM) ground states of the intradimer (interdimer) configuration. Figures 4(c) and 4(d) show the simulated STM images of the interdimer configuration on Br/Si(001) within the NM-buck and AFM structures, respectively. In contrast with H/Si(001), Br atoms appear brighter than DBs due to their relatively higher positions compared to those of H atoms. Our simulated filled-state image [Fig. 4(d)] of AFM agrees well with the room-temperature STM measurement⁸ where two DBs were imaged as nearly equal dark spots. Here, the observed symmetric image at room temperature may be due to the flipping motion of buckled dimers. Thus, future extremely low-temperature STM experiment could convincingly confirm our prediction that the interdimer configuration has an AFM ground state consisting of symmetric dimers.

In summary, we have theoretically predicted that two adjacent DBs on the H- and halogen-terminated Si(001) surfaces are antiferromagnetically coupled with each other. We hope that our predictions will stimulate spin-polarized STM experiments for direct identification of the AFM ground state of the interdimer configuration.

This work was supported by the Korea Science and Engineering Foundation grants of the Basic Research Program (No. R01-2006-000-10920-0) and the Korean government (MEST; Quantum Photonic Science Research Center).

*Corresponding author; chojh@hanyang.ac.kr

¹J. M. Jasinski, B. S. Meyerson, and B. A. Scott, *Annu. Rev. Phys. Chem.* **38**, 109 (1987).

²M. McEllistrem, M. Allgeier, and J. J. Boland, *Science* **279**, 545 (1998).

³U. Höfer, L. Li, and T. F. Heinz, *Phys. Rev. B* **45**, 9485 (1992).

⁴M. Dürr and U. Höfer, *Surf. Sci. Rep.* **61**, 465 (2006).

⁵M. Dürr, A. Biedermann, Z. Hu, U. Höfer, and T. F. Heinz, *Science* **296**, 1838 (2002).

⁶C. H. Schwalb, M. Lawrenz, M. Dürr, and U. Höfer, *Phys. Rev. B* **75**, 085439 (2007).

⁷B. R. Trenhaile, V. N. Antonov, G. J. Xu, K. S. Nakayama, and J. H. Weaver, *Surf. Sci. Lett.* **583**, L135 (2005).

⁸K. S. Nakayama, E. Graugnard, and J. H. Weaver, *Phys. Rev. Lett.* **89**, 266106 (2002).

⁹E. Pehlke, *Phys. Rev. B* **62**, 12932 (2000).

¹⁰Y. Kanai, A. Tilocca, and A. Selloni, *J. Chem. Phys.* **121**, 3359 (2004).

¹¹T. Hitosugi, S. Heike, T. Onogi, T. Hashizume, S. Watanabe, Z.-Q. Li, K. Ohno, Y. Kawazoe, T. Hasegawa, and K. Kitazawa, *Phys. Rev. Lett.* **82**, 4034 (1999).

¹²R. A. Wolkow, *Phys. Rev. Lett.* **68**, 2636 (1992).

¹³P. Hohenberg and W. Kohn, *Phys. Rev.* **136**, B864 (1964); W. Kohn and L. Sham, *ibid.* **140**, A1133 (1965).

¹⁴J. P. Perdew, K. Burke, and M. Ernzerhof, *Phys. Rev. Lett.* **77**, 3865 (1996); **78**, 1396(E) (1997).

¹⁵N. Troullier and J. L. Martins, *Phys. Rev. B* **43**, 1993 (1991).

¹⁶S. B. Healy, C. Filippi, P. Kratzer, E. Penev, and M. Scheffler, *Phys. Rev. Lett.* **87**, 016105 (2001).

¹⁷E. Artacho and F. Yndurain, *Phys. Rev. Lett.* **62**, 2491 (1989).

¹⁸M. R. Radeke and E. A. Carter, *Phys. Rev. B* **54**, 11803 (1996); J. Shoemaker, L. W. Burggraf, and M. S. Gordon, *J. Chem. Phys.* **112**, 2994 (2000).

¹⁹The spin-polarized pseudopotential DFT theory has been successfully used to describe magnetic orderings in several C- and Si-based systems such as honeycomb sheets consisting of B, N, and C atoms [S. Okada and A. Oshiyama, *Phys. Rev. Lett.* **87**, 146803 (2001)]; C nanotube [N. Park *et al.*, *ibid.* **91**, 237204 (2003)]; H-deposited Si(111) surface [S. Okada *et al.*, *ibid.* **90**, 026803 (2003)]; and graphite [P. O. Lehtinen *et al.*, *ibid.* **93**, 187202 (2004)].

²⁰C. F. Bird and D. R. Bowler, *Surf. Sci. Lett.* **531**, L351 (2003).

²¹L. Noodleman, *J. Chem. Phys.* **74**, 5737 (1981).

²²M. Dürr, Z. Hu, A. Biedermann, U. Höfer, and T. F. Heinz, *Phys. Rev. Lett.* **88**, 046104 (2002).

²³J. Tersoff and D. R. Hamann, *Phys. Rev. Lett.* **50**, 1998 (1983); *Phys. Rev. B* **31**, 805 (1985).

²⁴We found that the peak-to-valley height difference in the filled-state image of AFM changes from 0.47 to 0.37 Å as the simulated charge density decreases from 7×10^{-5} to 7×10^{-6} electrons/Å³.